OPEN ACCESS
IOP Publishing
Journal of Physics G: Nuclear and Particle Physics
J. Phys. G: Nucl. Part. Phys. **51** (2024) 075106 (13pp)
https://doi.org/10.1088/1361-6471/ad4efe

New measurements of the $^{19}F(p,\alpha_0)^{16}O$ and $^{19}F(p,\alpha_\pi)^{16}O^*$ reaction cross sections close to the Coulomb barrier

L Redigolo[1,2,*], I Lombardo[1,2], D Dell'Aquila[3,4], A Musumarra[1,2], M G Pellegriti[2], M Russo[1,2], G Verde[2] and M Vigilante[3,4]

[1] Dipartimento di Fisica e Astronomia, Università degli Studi di Catania, via S. Sofia 64, I-95123, Catania, Italy
[2] INFN—Sezione di Catania, via S. Sofia 64, I-95123, Catania, Italy
[3] Dipartimento di Fisica 'Ettore Pancini', Università degli Studi di Napoli 'Federico II', via Cinthia 21, I-80126, Napoli, Italy
[4] INFN—Sezione di Napoli, via Cinthia 21, I-80126, Napoli, Italy

E-mail: luigi.redigolo@ct.infn.it and ivano.lombardo@ct.infn.it

Received 15 March 2024, revised 2 May 2024
Accepted for publication 22 May 2024
Published 12 June 2024

Abstract

New absolute cross section measurements of the $^{19}F(p,\alpha_0)^{16}O$ and $^{19}F(p,\alpha_\pi)^{16}O^*$ reactions at energies close to the Coulomb barrier are reported. The availability of high-resolution and low-noise energy spectra obtained in the experiment allowed to resolve the 6.05–6.13 MeV doublet in ^{16}O. In particular, the α_π channel cross section was measured in the poorly-known 1.3 MeV bombarding energy region, and the α_0 channel was investigated in the 1.6 MeV region, where a strong discrepancy between previous data-sets is present. A comprehensive *R*-matrix fit, including the new data, was performed and the structure of the states ranging in the 14–15 MeV region is discussed.

Keywords: nuclear reaction, spectroscopy of neon 20, alpha clustering, absolute cross section measurement

* Author to whom any correspondence should be addressed.

1. Introduction

The ^{19}F(p,α)^{16}O reaction began to acquire importance in the '30s, when John Cockroft and Ernest Sinton Walton [1] started to study the emission of energetic α particles as the effect of transmutations induced in fluorine targets by an impinging proton beam; other pioneering studies on this subject are described, e.g. in [2–4]. At low bombarding energies, this reaction mainly proceeds through the formation of the ^{20}Ne compound nucleus. Following the historical notations (see, e.g. [4–7]), the $\alpha + {}^{16}$O emission channels will be indicated with the α_0 and α_π symbols when, respectively, the ^{16}O residual nucleus is left in its ground state or in the first (6.049 MeV, 0^+) excited state. The latter de-excites to the ground state by pair emission, and it is characterized by pronounced $4p-4h$ configurations linked to a possible $\alpha+{}^{12}$C cluster structure [8].

In the '40–'80s period, this reaction was widely explored in a broad energy range ($\approx$0.5$-$10 MeV), mainly to probe the structure of the ^{20}Ne compound nucleus [3, 4, 6, 9–11]. Nowadays, this reaction acquired importance also in the nuclear astrophysics field: its cross section knowledge could help to solve the puzzle of the fluorine nucleosynthesis in asymptotic giant branch (AGB) stars [12–14]. Furthermore, the balance between ^{19}F(p,α)^{16}O and ^{19}F(p,γ)^{20}Ne reaction rates can play an important role in escape pathways from the CNOF cycle, leading to nucleosynthesis of heavy elements (up to Ca) in very old stars [15–17].

On the nuclear structure side, further investigations of the α_0 and α_π channels may help to highlight the occurrence of cluster structures in ^{20}Ne above the proton separation energy (12.844 MeV) and the closely-lying $2\alpha+{}^{12}$C cluster decay threshold [18]. Parity and angular momentum considerations imply the exclusive population of natural parity states. Moreover, it can be easily demonstrated [6] that the orbital angular momentum in the entrance channel $\ell_{\rm in}$ must be equal to the orbital angular momentum in the outgoing channel $\ell_{\rm out}$ and then to the angular momentum J of the resonant state. This means that, by performing ^{19}F(p,$\alpha_{0,\pi}$)^{16}O reactions at quite low bombarding energy, a further selectivity towards the population of low J states in ^{20}Ne is thus expected. This feature can be quite important to unveil the presence of a particular class of α cluster 0^+ states, the so called *quartet excitations*, predicted in [19] to exist also at large excitation energies ($\approx$13–16 MeV). Considerations of this type were also driven by the key role played by the ^{16}O nucleus in the investigation of shape coexistence properties; in fact, as proposed in [20] and recently highlighted in [21], the first excited 0^+ state of this nucleus is characterized by a large deformation. Similarly, there is still an open question on the possible quartet nature of the 14.47 and 14.92 MeV 0^+ states [10, 22]. For the former, a completely different interpretation was also proposed: it could be, in fact, a $T=1$ iso-analogue of the 4.435 MeV state in ^{20}F [11]. All these questions still need to be clarified.

In the last years, the renewed interest on this reaction led to new experimental measurements (see, e.g. [23–26]) and theoretical interpretations (see, e.g. [27]). Nevertheless, some lacking of data and/or the presence of conflicting results are still observed in some energy regions of both the α_0 (around 1.6 MeV) and α_π (around 1.3 MeV) excitation functions (e.g. see the discussions of [28, 29]).

In this framework, the two-fold aim of the present work was (1) to study the α_π channel in the poorly known 1.1–1.3 MeV center of mass energy region, and (2) to investigate the α_0 channel cross section at $E_{\rm cm} \approx$ 1.6–1.7 MeV, where previous data strongly disagree. In fact, in this energy region, the cross section data previously reported in the literature [10, 30], even after the accurate normalization procedure described in [28], are different by a factor $\approx$1.5: this represents the main discrepancy existing in the ^{19}F(p, α_0)^{16}O data, which prevents the unambiguous partial widths determination for the 0^+ state at 14.47 MeV (and its neighbors) in ^{20}Ne. It is worth noting that the measurement of the α_π channel spectra is particularly

challenging: in ^{16}O, the 6.049 MeV state is very close to the 6.130 MeV state [31]. Thus, very high-resolution and low-background spectra are needed to resolve the doublet.

The manuscript is organized as follows: the experimental setup is described in section 2, while the method adopted to determine the absolute cross sections for both the reaction channels, by means of an internal normalization procedure, is described in section 3. The obtained cross sections were then compared with the previous measurements reported in the literature. In section 4, the newly obtained cross sections are included in a comprehensive *R*-matrix fit procedure, involving a large variety of reaction channels. As a result, a new set of reduced partial widths was determined for excited states in ^{20}Ne at $E_x \approx 14-15$ MeV, and some considerations on the structure of such states are drawn.

2. Experimental setup

The experiment was performed at the Singletron accelerator of the University of Catania (Italy), using proton beams in the bombarding energy windows of 1.13–1.30 MeV and 1.62–1.72 MeV. The beam energy stability was better than 1 keV, and the average beam intensity was about 100 nA. The beam spot on the target was of the order of 2 mm^2. To obtain the excitation functions and angular distributions of the cross sections, the projectile energy was varied in 10 or 20 keV steps, while the angular position of the detector was varied between 115 and 165 degrees, with 10 degrees angular steps. The uncertainty in the determination of the central polar angle of detection was one prime, while the angular opening of the collimated detector was about one degree. The target was made of a calcium fluoride film, 30 μg cm^{-2} thick, deposited over a carbon backing with 10 μg cm^{-2} thickness. The thicknesses of the layers in the target were measured, with an accuracy of ≈5%, by the energy loss of 5.486 MeV 241-Am α particles in each layer, before and after the evaporation. To prevent carbon build-up and deposition effects on the target, the vacuum level in the experimental chamber was better than 10^{-7} mbar. A tri-dimensional representation of the experimental apparatus is given in figure 1.

The energy of the accelerated beam was carefully cross-checked by means of a dedicated calibration procedure, scanning in fine steps a bench-marked anti-resonance profile seen in the differential cross section of p+^{12}C elastic scattering events at energies between 1.6 and 1.7 MeV and $\theta_{\rm lab} = 165°$ [32]. In doing this procedure, the p+^{12}C elastic scattering cross sections (in relative units) were determined by two independent methods: by internal normalization of the p+^{12}C yields to the Rutherford cross-section associated to p+^{40}Ca events, and by direct estimates making use of the integrated current. Both methods lead to calibration curves (expressed as excitation functions) which are in excellent agreement with literature data, with discrepancies much smaller than 1 keV.

The detection of charged particles was achieved by using a silicon detector, similar to the ones used in [23, 25, 33]. The front-end electronics included a low-noise charge pre-amplifier, followed by a spectroscopic amplifier. Particular care was dedicated in tuning all the amplifier parameters, especially to the pile-up rejection. The obtained energy resolution was 0.3% at 5 MeV. The energy calibration of the detector was obtained by using a triple-nuclide mixed α source and proton elastic scattering points on various elements present in the target (taking into account the energy losses of beam and outgoing particles); the observed linearity was excellent ($1 - R^2 \simeq 6 \times 10^{-6}$) in the entire calibration energy range (≈1–6 MeV). The beam current was collected by using the whole insulated vacuum chamber as a Faraday cup; considering the geometry of the beam line and the chamber, the charge losses due to possible escape of backward-emitted electrons are negligible.

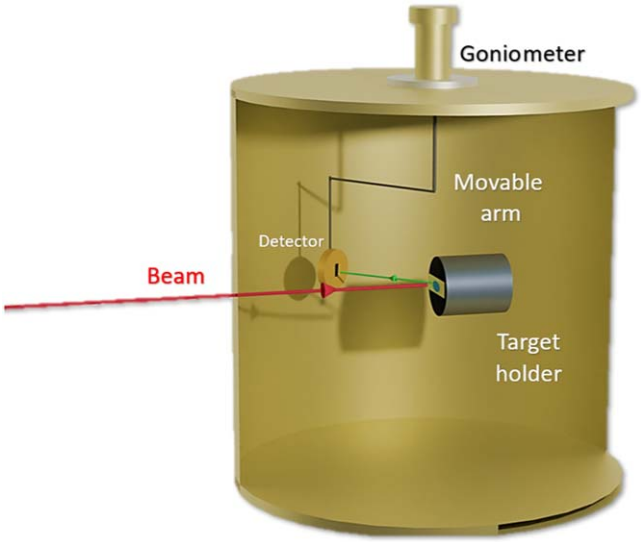

Figure 1. Three-dimensional cutaway representation of the reaction set-up. The proton beam is indicated in red, while the path of the detected particles to the detector is shown in green.

3. Experimental results and comparisons with previous data-sets

A typical ejectile energy spectrum obtained at 1.2 MeV bombarding energy and $\theta_{lab} = 165°$ is shown in figure 2. The obtained energy resolution of the α_π peaks is a factor $\approx$1.3 better than in [34], allowing an excellent separation of the α_π yields from the neighboring α_1 peak.

In the first window of the panel, it is possible to note how the elastic peaks are very well separated. The counts under the peaks, for each reaction event, were obtained through a multi-gaussian fit. A polynomial contribution was included in the fit, only in the elastic peaks region, to describe the (small) observed background.

Under bombardment, it could be possible to observe sizable variations on the fluorine content and stoichiometry in the CaF_2 target (see, e.g. the extended discussions reported in [35, 36]) that could consequently misrepresent the determination of the cross section. To overcome this problem, a careful internal normalization procedure has been adopted in the present work, by dividing the α_0 and α_π yields to the p+^{19}F elastic yields obtained in the same experimental conditions, as similarly done, e.g. in [37]. In this framework, the absolute p+^{19}F elastic scattering differential cross sections (DCS) were extrapolated from the *R*-matrix fit of [29]. The extrapolation describes very well the experimental absolute DCS data at 135° and 145° from [34] and at 153° from [38]; such experimental DCS have been recently bench-marked in [39]. Statistical uncertainties were estimated by standard error propagation, including the statistical uncertainty on the counting rate; a 10% non-statistical uncertainty in the determination of the p+^{19}F elastic scattering DCS was assumed by considering the typical deviations observed between the bench-marked data sets used in [39].

In the limit of thin target and small detection solid angles, considering the vanishing possibility of multiple collisions, the DCS for the α_0 and the α_π channels were obtained by using the following expression, where $\frac{d\sigma}{d\Omega}^{p,\mathrm{ela}}$ is the elastic scattering DCS, $N_{\alpha_{0,\pi}}$ and $N_{p,\mathrm{ela}}$ are respectively the $\alpha_{0,\pi}$ channel counts and the p + ^{19}F elastic counts on the same detector:

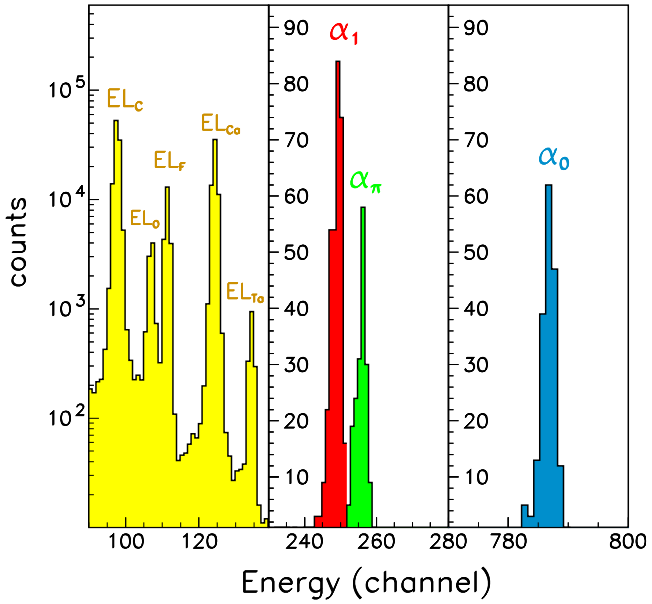

Figure 2. Energy spectra of the ejectiles emitted at $\theta = 165°$ when a proton beam of $E_{\rm lab} = 1.2$ MeV energy impinged on the CaF_2 (on carbon backing) target used in the present experiment. Horizontal and vertical scales were separated, as a function of the ejectile energy, for clarity reasons. Elastic peaks on C, O, F, Ca and Ta are shown in yellow, with a logarithmic y-scale. The presence of Ta contaminants in the target is due to the tantalum crucible used to evaporate the CaF_2 layer, which has very high melting and boiling points. Peaks due to the α_1, α_π and α_0 channels are respectively shown in red, green and light blue, with a linear count scale.

$$\frac{\mathrm{d}\sigma}{\mathrm{d}\Omega}^{\alpha_{0,\pi}}(\theta, E) = \frac{N_{\alpha_{0,\pi}}}{N_{p,\mathrm{ela}}} \cdot \frac{\mathrm{d}\sigma}{\mathrm{d}\Omega}^{p,\mathrm{ela}}.$$

This method allows to determine the absolute DCS for the α_π and the α_0 channels independently from the possible fluorine content variation in the target. A relativistic Jacobian transformation was then applied to obtain the absolute DCS in the center of mass frame. In figure 3 some DCS are reported for both the reaction channels as a function of bombarding energy and at different polar angles.

In figure 4, the excitation function $\frac{\mathrm{d}\sigma}{\mathrm{d}\Omega_{\rm lab}}$ obtained at $\theta_{\rm lab} = 155°$ was then compared to previous datasets obtained at $\theta_{\rm lab} = 150°$ [40, 41]. Data from the present work are in agreement, within the error bars, with the ones reported by [40]. As it was also suggested in [40], a scale factor of 2 was applied to data of [41] to match the two cross section scales. It is worth noting that a similar scaling factor was already used in the past to match the cross section scales of data from [23] and [41] at lower energies.

Since the present data were collected in the backward hemisphere, it is necessary to know the shape of angular distributions in the whole range of polar angles, in order to obtain the integrated cross sections for each energy. Such information can be derived from previous works (as [6] and [5]), in relative units or as Legendre-polynomial expansions, for both channels. The angular distribution shapes were then extrapolated at the energies of interest from [5, 6] through spline fits of B_i, the coefficients of Legendre polynomial expansions of the angular distributions, truncated to the fourth-order (i.e. considering the *d*-wave as the highest

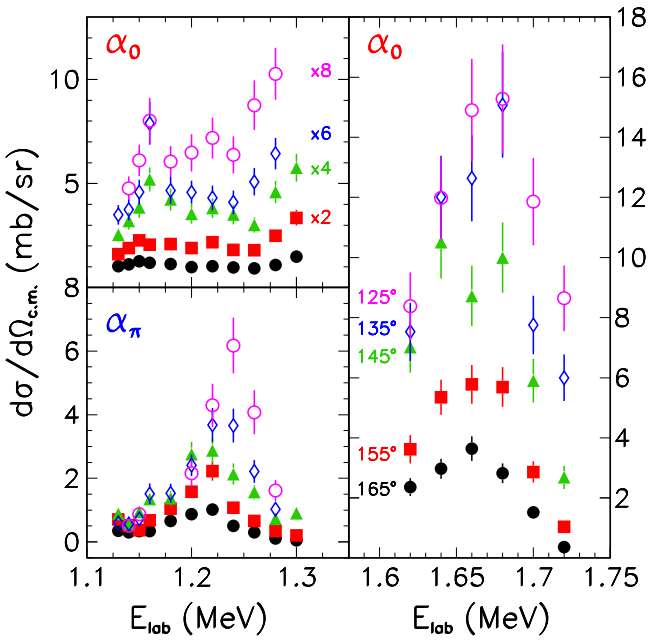

Figure 3. Excitation functions $\left(\frac{d\sigma}{d\Omega_{cm}}\right)$ obtained from the present work, for the α_0 (Top Left panel: $E_{lab} \simeq 1.1$-1.3 MeV; right panel: $E_{lab} \simeq 1.6$–1.72 MeV) and the α_π (bottom left panel: $E_{lab} \simeq 1.1$–1.3 MeV) channels, shown at different polar angles in the laboratory reference frame. Horizontal error bars are smaller than symbols sizes. The energy resolution is around 1 keV in the explored range. For clarity reasons, different scaling factors have been used for data at various polar angles, as indicated in the top left panel: these were, respectively, 2, 4, 6 and 8 for the 155°, 145°, 135° and 125° data.

partial wave contributing to the cross section, as discussed in [5, 29, 30, 34]). Then, the integrated cross sections were estimated, together with their uncertainties, for the $\alpha_{0,\pi}$ channels from the equation $\sigma(E) = A(E) \cdot 4\pi B_0(E)$. $A(E)$ is a scaling parameter obtained by fitting this work's (absolute) angular distributions at backward angles to the overall angular distribution shapes (in relative units) extrapolated from [5, 6]. Some examples of these normalization fits can be seen in figure 5. A good agreement between the present data and the trends previously reported in the literature (red and blue lines), is observed for both reaction channels.

Concerning the α_π channel, the integrated cross section data obtained in the present experiment are reported as black dots in figure 6. Green triangles refer to data obtained at the INFN-LNL (Legnaro, Italy) [10] and TTT3 tandem (Naples, Italy) [42] accelerators during the '70s; the integrated cross section coming from such data were already reported in [29]. A good agreement (within ≈2 standard deviations) between the two data sets is evident, with the exception of a slight energy shift, smaller than 10 keV, at $E_{cm} > 1.15$ MeV.

Concerning the α_0 channel, the attention was focused on the $E_{cm} \simeq 1.5$–1.8 MeV region, where, even after applying a careful normalization based on several existing data-sets (see [28]), a sizable discrepancy is still present between data coming from [10, 30]. In figure 7, the present integrated cross section data are displayed (black dots), together with data from [10] (red triangles) and [30] (light blue squares). The obtained data are in excellent agreement with the ones of [10] (within $\approx 1.7\sigma$); much larger discrepancies (between $\pm 3.5\sigma$) are obtained by

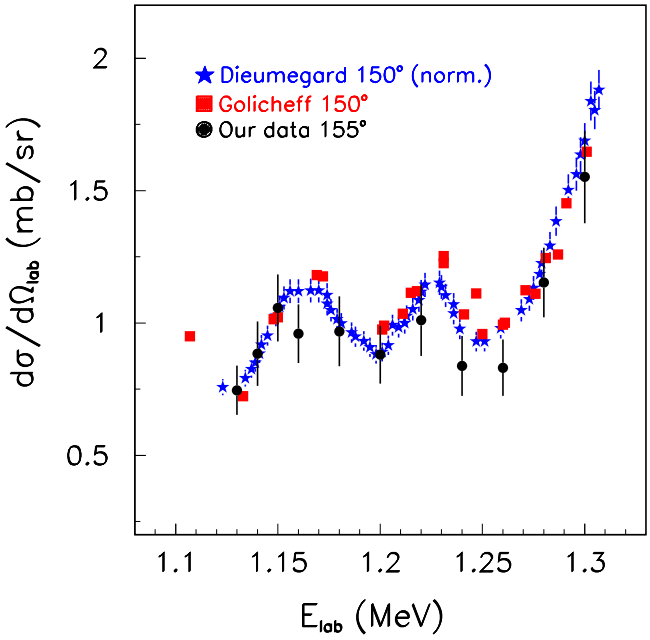

Figure 4. Excitation function $\frac{d\sigma}{d\Omega_{lab}}(E_{lab})$ at 155° obtained from the present work (black dots) and those from [40] (red squares; experimental uncertainty not indicated in the original work) and [41] (blue stars, normalized as discussed in the text).

comparing this work's data to the ones of [30] (as normalized in [28]). A possible origin of the difference between the two existing datasets may be linked to the different shapes of angular distributions (at $E_p \approx 1.7$ MeV) reported and/or to efficiency effects in evaluating the integrated current in [30].

4. Considerations on the structure of ^{20}Ne at high excitation energies

To improve the spectroscopic knowledge of the excited states of the ^{20}Ne compound nucleus in the $E_x \simeq 13.7-14.8$ MeV region and, consequently, to draw some considerations on its structure, a comprehensive *R*-matrix fit was performed, including the α_0 and α_π data obtained in this measurement. The fitting procedure was applied to the same database of [29], with the addition of the integrated cross section data coming from the present work for the α_π channel in the $E_{cm} \simeq 1.07-1.24$ MeV region, and for the α_0 channel in the $E_{cm} \simeq 1.54-1.62$ MeV range. Furthermore, in the $E_{cm} \simeq 1.54-1.72$ MeV region (green hatched area in figure 8, upper panel), the α_0 integrated cross section data by [10] were included in the fit, considering their coherence with the present measurements, while the data from [30] were excluded. The starting resonance parameters (E_x, total and partial width values) adopted in the fit were taken from [29]. J^π values were fixed to the ones of [29], that were in good agreement with the systematic reported in [18].

The results of the new *R*-matrix fit are shown in figure 8 as red solid lines; blue dashed lines reports the previous fit of [29]. Only results for the α_0 and α_π integrated cross section for $E_{cm} = 1-2$ MeV are displayed, while the fits to the other included data ([29] database) give nearly the same results of [29] and are not shown for simplicity.

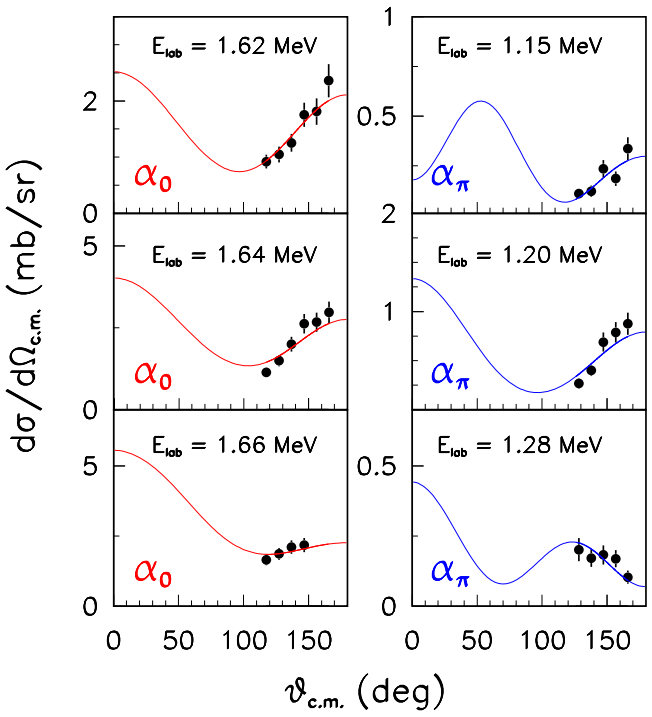

Figure 5. Angular distributions (black dots) of the ^{19}F(p,α_0)^{16}O (left panels) and ^{19}F(p, α_π)^{16}O* (right panels) reactions investigated in the present work. Red and blue solid lines represent the shape of angular distributions reported in [5, 6], normalized to the present absolute cross sections data obtained in the backward hemisphere at some bombarding energies.

From the present *R*-matrix fit, it is possible to recognize a small shift in the energy of the peaks seen at $E_{\rm cm} \simeq 1.07-1.15$ MeV in the α_π integrated cross section and, mainly, a strong change in the shape and amplitude of the large peak seen in the α_0 cross section at $E_{\rm cm} \simeq 1.6$ MeV. Table 1 shows the new parameters (excitation energies, total and partial widths) obtained from the present fit for states in the excitation energy region $E_x \approx 13.8-14.7$ MeV; such values are compared with the corresponding ones reported in [29].

In general, the positions of excited states agree with the literature values within about 20 keV, and the total and partial widths are in most cases in agreement with the previous values within ≈10%, essentially confirming the results reported in [29]. Some interesting deviations are seen for the 13.93 MeV state, only involved in the α_0 and p_0 channels, for which the Γ_{α_0} partial width is ≈40% larger than the previously reported values.

Concerning the 13.92 MeV 2^+ state, the new data of the α_π channel lead to sizable change in the total and partial widths; the total width is almost doubled, reaching a value (53.4 keV) very close to the one reported in the compilation of [18] (48 keV); the Γ_{α_π} partial width is approximately two times the previously reported value of [29]. The Γ_{p_0} value is also a factor ≃2 larger than the one of [29], going towards a better agreement to the old value reported by Isoya (57 keV, [6]). Differences are also seen in the partial widths of the 14.02 MeV 1^- state, which shows a $\frac{\Gamma_{\alpha_\pi}}{\Gamma_{\alpha_0}}$ branching ratio close to unity; a similar branching was also reported by [6].

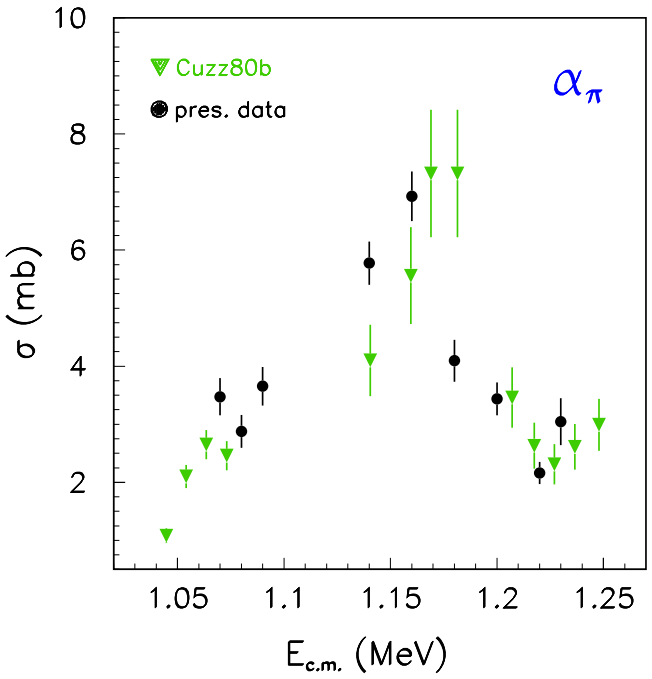

Figure 6. Integrated cross section for the ^{19}F(p,α_π)^{16}O* reaction in the energy region $E_{cm} \simeq 1-1.3$ MeV. Present results are shown as black full dots, while green downward oriented triangles indicate previous unpublished results from [42] (Cuzz80b) as reported and discussed in [29].

Table 1. Spectroscopic parameters for states in ^{20}Ne determined from the present *R*-matrix fit, contributing in the energy region explored in the present experiment, i.e. $E_{cm} \simeq 1.0$–1.7 MeV. Parameters for the 15.419 MeV state are also included because they are recalled in section 4. Present values are compared with the previous ones from [29]. Excitation energy values E_x are given in MeV. The total (Γ_{cm}) width and α partial widths (Γ_{α_0}, Γ_{α_π}) are given in keV, while the proton partial widths Γ_{p_0} are expressed in the units indicated in the text.

J^π	$E_x^{[prev.]}$	E_x	$\Gamma_{cm}^{[prev.]}$	Γ_{cm}	$\Gamma_{\alpha_0}^{[prev.]}$	Γ_{α_0}	$\Gamma_{\alpha_\pi}^{[prev.]}$	Γ_{α_π}	$\Gamma_{p_0}^{[prev.]}$	Γ_{p_0}
...	...	...	...	...	...	...	...	...	...	...
1^-	13.89	13.89	293	303	162	157	17	16.4	447 eV	537 eV
2^+	13.910	13.927	29	53.4	8	12.7	21	40.6	21 eV	39 eV
0^+	13.912	13.932	251	351	251	351	0	0	381 eV	563 eV
1^-	14.02	13.992	61	49	6	23.5	55	25.4	189 eV	140 eV
2^+	14.131	14.131	39	36.5	33	32	6	4.1	405 eV	368 eV
1^-	14.351	14.352	151	127	42	25	108	101	1.0 keV	877 eV
0^+	14.466	14.450	96	99	64	69.5	25	16.2	7.0 keV	13.5 keV
1^-	14.596	14.596	287	315	212	230	65	75.5	9.8 keV	9.6 keV
0^+	14.653	14.653	160	148	143	133	11	8.1	6.5 keV	6.9 keV
...	...	...	...	...	...	...	...	...	...	...
2^+	15.419	15.419	60	60	29	29	29	29	63 eV	63 eV
...	...	...	...	...	...	...	...	...	...	...

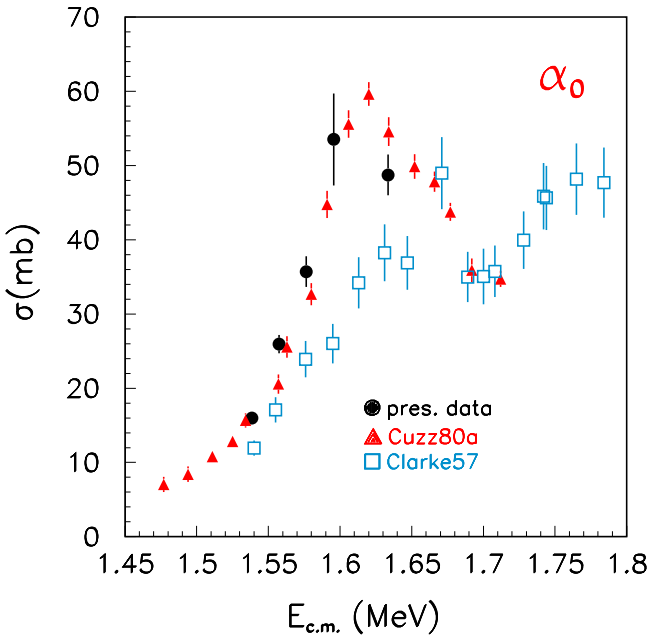

Figure 7. Comparison of integrated cross sections (σ) between present data (black dots) and those from [10] (Cuzz80a, red triangles) and [30] (Clarke57, light blue boxes, normalized as discussed in [28]) for the ^{19}F(p, α_0)^{16}O reaction in the energy region $E_{\rm cm} \simeq 1.45-1.75$ MeV.

The most interesting information comes out for the 0^+ state at $E_x \simeq 14.47$ MeV. [22] indicates this state as the head for the [*211*] quartet band; [10] instead suggested the 14.92 MeV 0^+ state as the [*211*] band-head, assigning a possible [*220*] structure to the 14.47 MeV one. On the other hand, [11] indicates that this state could be the iso-analogue of the 4.315 MeV, $T = 1$, 0^+ state in ^{20}F, which does not show a quartet configuration.

In figure 8 one can observe that this state is responsible for the pronounced peaks seen at $E_{\rm cm} \simeq 1.61$ MeV in the integrated cross sections of both reaction channels: the conflict between data of [10, 30] has therefore prevented a solid spectroscopic analysis. The present reduced widths, reported in table 1, show a small p_0 branching ratio, $\frac{\Gamma_{p0}}{\Gamma} \simeq 0.14$, in contrast with the very large value $\frac{\Gamma_{p0}}{\Gamma} \simeq 0.79$ reported in [11]. The occurrence of a $\frac{\Gamma_{p0}}{\Gamma}$ branching ratio much smaller than 0.79 was also reported in a recent fit involving only elastic scattering data ([39], $\frac{\Gamma_{p0}}{\Gamma} \simeq 0.40$). The present Γ_{p_0} value leads to a spectroscopic factor ≈4–5 times smaller than the one experimentally observed for the 4.315 MeV state in ^{20}F [43, 44], in disagreement with the hypothesis of an iso-analogue state.

Furthermore, as discussed in [10, 22], the presence of reduced partial widths $\gamma^2_{\alpha_\pi} > \gamma^2_{\alpha_0}$ could point out the occurrence of a quartet state in ^{20}Ne of the [*211*] or [*220*] type. In this framework, it was firstly suggested in [22] that the 14.47 MeV state could have a quartet structure, because of their estimate of reduced partial widths: $\frac{\gamma^2_{\alpha_\pi}}{\gamma^2_{\alpha_0}} \approx 1.6$. In the present analysis, a smaller value of the ratio of the partial widths was found $\left(\frac{\gamma^2_{\alpha_\pi}}{\gamma^2_{\alpha_0}} \approx 1\right)$ not supporting the quartet structure previously suggested.

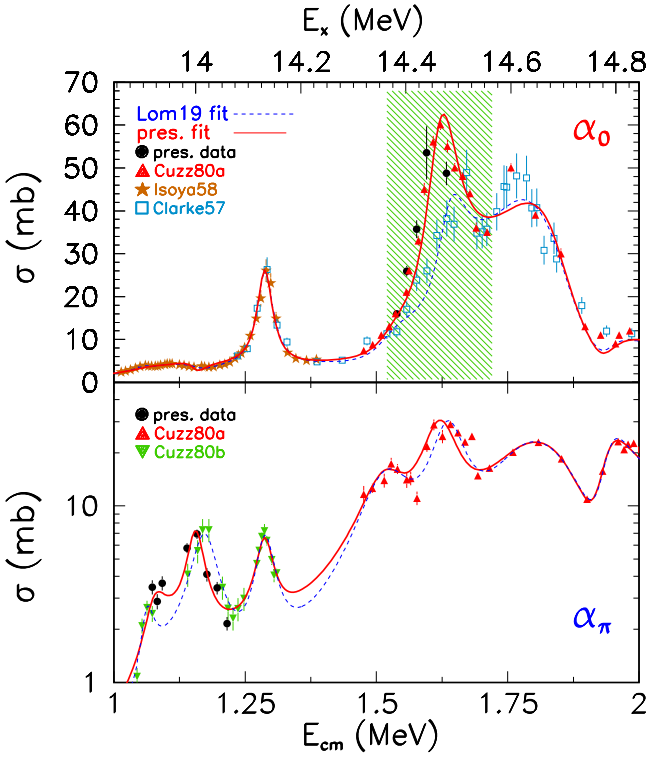

Figure 8. *R*-matrix fit to present data (red solid lines), together with other data previously reported in the literature. (Upper panel) Integrated cross section for the α_0 reaction channel. Black dots: present data. Literature data, as normalized in [28], are displayed as follows: red upwards triangles are data from [10]; brown stars are data from [6]; light blue boxes are data from [30]. Blue dashed line: *R*-matrix fit from [29]. Inside the green hatched box, only present data and data from [10] were included in the fit. (Lower panel) Integrated cross section for the α_π reaction channel. Green downwards triangles refer to data from [42], as reported in [29]. Blue dashed line: *R*-matrix fit from [29].

At variance, the present analysis and [29] indicates the [*211*] quartet nature of the 14.92 MeV state, for which the dimensionless reduced partial width of the α_π channel is dominant over the p_0 and α_0 channels, in agreement with the old conclusions of [10]. This finding suggests some interesting, even if simplified, speculations. The [*211*] quartet state should have, in fact, a pronounced ^{12}C+2α cluster structure [10, 19]. If we assume the clusters as homogeneous spheres touching at their surfaces, it is possible to (roughly) estimate the inertial parameter of such configuration as $\frac{\hbar^2}{2\mathcal{I}} \approx$ 70–90 keV. Therefore, a possible 2^+ rotational excitation of the 14.92 MeV quartet state should be located at $E_x \approx 15.3-15.4$ MeV. Indeed, both the present work and [29] reported the presence of 2^+ states in this energy window. In this context, the state at 15.419 MeV is a promising candidate: its reduced partial width for the α_π channel is well larger than the one for the α_0 ($\gamma^2_{\alpha_\pi} \simeq 10$ keV, $\gamma^2_{\alpha_0} \simeq 2.7$ keV), and both are much larger than the one for the p_0 channel (few tenths of keV), a pattern quite similar to the one observed for the 14.92 MeV state. These speculations strongly call for further experiments, including the ones studying the elusive ^{8}Be+^{12}C cluster decay in ^{20}Ne [45].

5. Conclusions

This paper reports results on a new experiment aiming to study the ^{19}F(p,α)^{16}O reaction at low bombarding energies, using very high-quality beams delivered by a Singletron accelerator, and state-of-the-art solid state detectors. This allowed to clearly separate the contributions coming from the ^{16}O doublet at 6.049–6.13 MeV. Particle yields were transformed into absolute differential cross sections by means of an accurate internal normalization procedure based on the use of bench-marked elastic scattering data. Differential cross sections were then integrated in the whole angular domain by considering the trends of angular distributions reported in the literature.

This experiment had two main goals: to provide new data in the poorly known energy region of $E_{\rm cm} \approx 1.1$ MeV for the α_π channel, and to investigate the discrepancy still persisting in the literature between the data of [10] and [30] in the α_0 reaction channel. Concerning the last point, the present data clearly agree with the ones of [10]; a possible explanation for the existing discrepancy between the datasets [10, 30] is also outlined.

The availability of new cross section data allows to refine the *R*-matrix fit of several reaction channels reported in [29]. As a result, nuclear structure information on natural-parity states in ^{20}Ne at $E_x \approx 13.9$–14.7 MeV was updated. In particular, the contrasting interpretations for the structure of the 14.47 MeV 0^+ state were disentangled, and a quartet structure for the 14.92 MeV 0^+ appears to be supported by the data here obtained. Qualitative considerations suggest that the 2^+ state at 15.42 MeV, reported in [29], could represent a rotational excitation of the quartet state at 14.92 MeV. If this hypothesis were true, the 14.92 MeV 0^+ state would be characterized by a very large deformation, given by its possible ^{12}C+2α structure. Further works, both from the experimental and theoretical side, are needed to shed light on this suggestion.

Acknowledgments

We are indebted to Prof. S Mirabella and Mr. S Tatì (Catania) for their support in the beam preparation and transport and for the set-up of the experiment at the Singletron laboratory of the University of Catania. We express our gratitude to Mr. M D'Andrea (INFN—Catania) for his continuous support during the preparation phase of the experimental set-up. I L, D D A, L R and M V gratefully acknowledge Profs. P Cuzzocrea, E Rosato (*deceased*) and E Perillo, G Spadaccini (Naples Federico II) for very useful discussions and suggestions about the study of the present reaction. I L and D D A thanks Profs. R J De Boer (Notre Dame) and J-J He (Beijing Normal) for several discussions on the subjects on this paper.

Data availability statement

All data that support the findings of this study are included within the article (and any supplementary files).

ORCID iDs

L Redigolo https://orcid.org/0000-0003-4623-469X
I Lombardo https://orcid.org/0000-0002-2686-9164
D Dell'Aquila https://orcid.org/0000-0001-5895-0664
M Russo https://orcid.org/0000-0003-3915-7833

References

[1] Cockcroft J D and Walton E T 1932 *Proc. R. Soc.* A **136** 619–30
[2] Henderson M C, Livingston M S and Lawrence E O 1934 *Phys. Rev.* **46** 38–42
[3] Burcham W and Smith C 1939 *Nature* **143** 795–6
[4] Streib J F, Fowler W and Lauritsen C 1941 *Phys. Rev.* **59** 253
[5] Isoya A, Goto K and Momota T 1956 *J. Phys. Soc. Jpn.* **11** 899–906
[6] Isoya A, Ohmura H and Momota T 1958 *Nucl. Phys.* **7** 116–25
[7] Barnes C 1955 *Phys. Rev.* **97** 1226
[8] Zuker A, Buck B and McGrory J 1968 *Phys. Rev. Lett.* **21** 39
[9] Burcham W E and Devons S 1939 *Proc. R. Soc.* A **173** 555–68
[10] Cuzzocrea P, de Rosa A, Inglima G, Perillo E, Rosato E, Sandoli M and Spadaccini G 1980 *Lett. Nuovo Cimento* **28** 515–22
[11] Ouichaoui S, Beaumevieille H, Bendjaballah N, Chami C, Dauchy A, Chambon B, Drain D and Pastor C 1985 *Nuovo Cimento* A **86** 170–82
[12] La Cognata M *et al* 2011 *Astrophys. J. Lett.* **739** L54
[13] La Cognata M *et al* 2015 *Astrophys. J.* **805** 128
[14] Indelicato I *et al* 2017 *Astrophys. J.* **845** 19
[15] Zhang L *et al* 2021 *Phys. Rev. Lett.* **127** 152702
[16] Zhang L *et al* 2022 *Nature* **610** 656–60
[17] De Boer R J *et al* 2021 *Phys. Rev.* C **103** 055815
[18] Tilley D R, Cheves C M, Kelley J H, Raman S and Weller H R 1998 *Nucl. Phys.* A **636** 249–364
[19] Arima A, Gillet V and Ginocchio J 1970 *Phys. Rev. Lett.* **25** 1043–6
[20] Morinaga H 1956 *Phys. Rev.* **101** 254
[21] Heyde K and Wood J 2016 *Phys. Scr.* **91** 083008
[22] De Rosa A, Perillo E, Cuzzocrea P, Inglima G, Rosato E, Sandoli M and Spadaccini G 1978 *Nuovo Cimento* A **44** 433–40
[23] Lombardo I *et al* 2013 *J. Phys. G: Nucl. Part. Phys.* **40** 1251102
[24] Nathanael A, Schmidt E, Wesch W and Wendler E 2015 *Nucl. Instrum. Methods Phys. Res., Sect.* B **345** 37–41
[25] Lombardo I *et al* 2015 *Phys. Lett.* B **748** 178
[26] Guardo G L *et al* 2023 *Eur. Phys. J.* A **59** 65
[27] Sahoo L K and Basu C 2021 *Int. J. Mod. Phys.* E **30** 2150102
[28] He J J *et al* 2018 *Chin. Phys.* C **42** 015001
[29] Lombardo I *et al* 2019 *Phys. Rev.* C **100** 044307
[30] Clarke R L and Paul E B 1957 *Can. J. Phys.* **35** 155–67
[31] Tilley D R *et al* 1993 *Nucl. Phys.* A **564** 1
[32] Mazzoni S, Chiari M, Giuntini L, Mandò P and Taccetti N 1998 *Nucl. Instrum. Methods Phys. Res., Sect.* B **136** 86–90
[33] Lombardo I *et al* 2013 *Nucl. Instrum. Methods Phys. Res., Sect.* B **302** 19
[34] Caracciolo R, Cuzzocrea P, De Rosa A, Inglima G, Perillo E, Sandoli M and Spadaccini G 1974 *Lett. Nuovo Cimento* **11** 33–8
[35] Couture A *et al* 2008 *Phys. Rev.* C **77** 015802
[36] Ugalde C, Azuma R, Couture A, Görres J, Lee H, Stech E, Strandberg E, Tan W and Wiescher M 2008 *Phys. Rev.* C **77** 035801
[37] Lombardo I *et al* 2021 *J. Phys. G.: Nucl. Part. Phys.* **48** 065101
[38] Knox J and Harmon J 1989 *Nucl. Instrum. Methods Phys. Res., Sect.* B **44** 40–2
[39] Paneta V, Gurbich A and Kokkoris M 2016 *Nucl. Instrum. Methods Phys. Res., Sect.* B **371** 54–8
[40] Golicheff I, Loeuillet M and Engelmann C 1974 *J. Radioanal. Nucl. Chem.* **22** 113–29
[41] Dieumegard D, Maurel B and Amsel G 1980 *Nucl. Instrum. Methods* **168** 93–103
[42] Cuzzocrea P *et al* 1980 *INFN/BE Report*
[43] Fortune H T, Morrison G C, Bearse R C, Yntema J L and Wildenthal B H 1972 *Phys. Rev.* C **6** 21–9
[44] Mosley C A J and Fortune H T 1977 *Phys. Rev.* C **16** 1697–702
[45] Gorodetzky P *et al* 1971 *J. Phys. Colloques* C **6** C197